Li^7 and Alpha Particles from the Li^6+Be^9 Reaction*

BALDEV SAHAI†
Department of Physics and The Enrico Fermi Institute for Nuclear Studies, The University of Chicago, Chicago, Illinois

(Received 25 August 1965)

The kinetic-energy spectra of Li^7 nuclei and alpha particles formed as a result of the nuclear reaction between Li^6 projectiles of energies 3.0–3.75 MeV and Be^9 targets have been studied by a particle-selection system using a gas proportional counter (ΔE) with a very thin window ($\sim$35 μg/cm^2) and solid-state detectors to measure the energy. No evidence could be found for discrete Li^7 energy groups such as would result from a two-product reaction producing Be^8 in its ground state or first excited state. The Li^7 spectrum is an energy continuum, whereas the alpha-particle spectrum has discrete energies as well as an energy continuum. Absolute values of $d^2\sigma/dE\,d\Omega$ have been obtained for these continua in the barycentric system. By extrapolation of the observed results, the total cross section σ_t for the Li^7 continuum is estimated to be 24$\pm$8 mb, whereas σ_t for the alpha continuum, which has contributions from some other reactions also, is estimated to be 103$\pm$30 mb. The reaction is interpreted as predominantly a direct three-body breakup $Be^9+Li^6 \rightarrow Li^7+2\alpha$ and sequential decay through highly excited states in B^{11}. Absolute differential cross sections for the four highest alpha groups from the concomitant reaction $Be^9(Li^6,\alpha)B^{11}$ are also given.

I. INTRODUCTION

THE studies on the reaction producing Li^7 when Be^9 is bombarded with a Li^6 ion beam have been prompted by the work[1–5] on the $Be^9(Li^7,Li^8)Be^8$ reaction. The latter has a Q value of 0.36 MeV, making it extremely difficult to observe the products directly. However, Li^8 is β-active with a half-life of 0.848$\pm$0.004 sec.[6] By measuring this radioactivity, Norbeck and Littlejohn[1] studied the cross section, and Norbeck *et al.*[2] studied the angular distribution of Li.[8] The latter work was done with bombarding energies of Li^7 up to 4.0 MeV. The angular distribution could be approximated as $\sin^2\theta$ in the center-of-mass system with the central peak shifting forward as the energy is increased. Allison[3] analyzed this reaction from the classical viewpoint. The reaction is treated as a neutron pickup from Be^9 by the passing Li^7 and it is assumed that owing to the low Q value of the reaction and relatively low mass of the neutron, Li^7 and Be^9 are not unrecognizably perturbed from the classical hyperbolic orbits they would follow under Coulomb repulsion. Comparison of the data and Rutherford-scattering calculations show that 1 in 10^6 of the passing Li^7 nuclei capture a neutron from Be^9 in encounters in which the perinuclear distance is as great as $(3.0\pm0.55)\times10^{-12}$ cm.

It is to be noted that the cross section for this reaction channel is one of the highest among the reaction channels which have been observed when Be^9 is bombarded with Li^7 at these energies, i.e., up to about 4.0 MeV.

It was therefore expected that Li^6 bombardment of Be^9 may also lead to a reaction going as $Be^9(Li^6,Li^7)Be^8$. We sought to observe Li^7 directly. When a Li^6 ion beam with a kinetic energy of 3.3 MeV is allowed to impinge upon a Be^9 target, quite a few reaction channel exits become available. Since in this paper we are interested only in those reactions in which alpha particles and Li^7 nuclei are produced, we list in Table I those reactions in which alpha particles and Li^7 nuclei with either discrete kinetic energies or with a continuum of kinetic energies can be produced and which have positive Q values.

TABLE I. Exothermic reactions yielding Li^7 and/or alpha particles.

Group A	
Reactions yielding Li^7 particles directly or indirectly	
$Li^6+Be^9 \rightarrow \alpha+B^{11}$	Q=14.347 MeV
$\rightarrow 2\alpha+Li^7$	Q= 5.681 MeV
$\rightarrow Li^7+Be^8$	Q= 5.587 MeV
Group B	
Other reactions yielding alpha-particle continua	
$Li^6+Be^9 \rightarrow 3\alpha+t$	Q= 3.215 MeV
$\rightarrow \alpha+n+B^{10}$	Q= 2.891 MeV
$\rightarrow \alpha+p+Be^{10}$	Q= 3.118 MeV
$\rightarrow \alpha+t+Be^8$	Q= 3.121 MeV

Of the reactions listed in Table I, Group A are those which can yield Li^7 of discrete or continuous kinetic energy, directly or indirectly. By using the word indirectly we imply, e.g., the production of Li^7 by de-excitation of some higher excited state in B^{11} since $B^{11} \rightarrow Li^7+\alpha$ has a $Q=-8.666$ MeV. Some of the higher excited states in B^{11} above and including the 8.923 MeV level are known to de-excite through alpha emission.[6]

* This work was supported in part by the U. S. Atomic Energy Commission.

† On leave of absence from Tata Institute of Fundamental Research, Bombay 5, India. The paper was submitted in partial fulfillment of the requirements for the Ph.D. degree.

[1] E. Norbeck, Jr., and C. S. Littlejohn, Phys. Rev. **108**, 754 (1957).
[2] E. Norbeck, J. M. Blair, L. Pinsonnealt, and R. J. Gebracht, Phys. Rev. **116**, 156 (1959).
[3] Samuel K. Allison, Phys. Rev. **119**, 1975 (1960).
[4] Robert J. Gebracht and Byron L. Youtz, Phys. Rev. **120**, 1738 (1960).
[5] C. W. Lewis, Phys. Rev. **131**, 2590 (1963).
[6] H. H. Landolt and R. Börnstein, *Tables, New Series* (Springer-Verlag, Berlin, 1961), Group 1, Vol. 1.

Group B lists all other reactions which can give rise to alpha continua in the observed charged-particle spectra.

II. APPARATUS AND EXPERIMENTAL PROCEDURE

A 3.75-MeV Van de Graaff accelerator installed at the Enrico Fermi Institute for Nuclear Studies during the year 1963 has been adapted to the acceleration of Li ion beams. The beam comes down vertically and is bent through 90° by a deflecting magnet. The latter was calibrated by using well-known resonances caused by proton and alpha-particle beams accelerated in the Van de Graaff accelerator. The beam energy spread in the experiments reported here is $\pm 0.5\%$ of the mean energy based on these measurements and the slit adjustments. The magnetic field (and hence the beam energy) can be measured quite accurately by the nuclear-magnetic-resonance technique.

Separated Li^6 with 99.3% enrichment in the initial stages and 99.99% at the later stages of the work was used for making Li^6 ion sources. This material was obtained from Oak Ridge National Laboratory. The preparation of the emitting material and the ion source have already been described by Allison and Kamegai.[7]

Thin, supported targets of Be^9 were used in some of the experiments. A method of preparation was adopted which made it easy to estimate the layer thickness. First an extremely thin layer of gold was evaporated onto the highly polished face of a nickel button. The beryllium layer was then deposited over the gold by evaporation, but a part of the target was shielded leaving the gold uncovered, as shown in Fig. 1. Several targets were thus prepared and bombarded with monoenergetic protons from a Cockcroft-Walton accelerator. The energies of the protons scattered at 90°

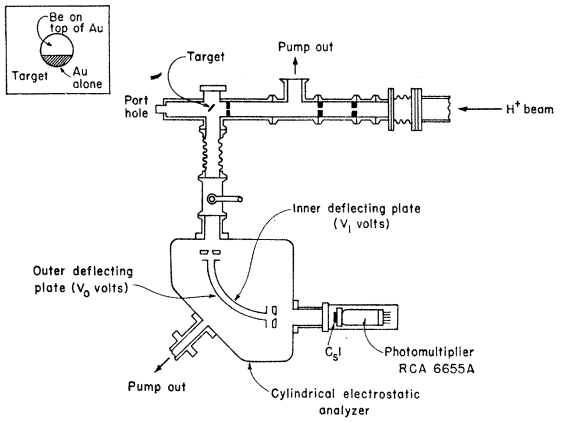

FIG. 1. Schematic drawing of the experimental arrangement used for target thickness measurements. The H^+ beam is generated in a Cockcroft-Walton accelerator. The inset gives a profile of the target surface.

[7] S. K. Allison and M. Kamegai, Rev. Sci. Instr. **32**, 1090 (1962).

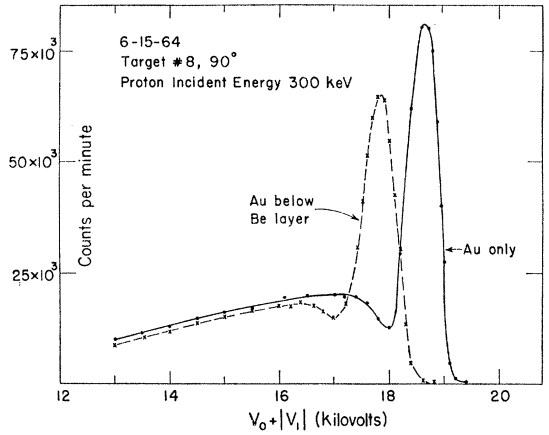

FIG. 2. Measurement of Be target thickness. The peaks show scattered protons from a thin gold layer on a nickel button. The solid curve shows the scattering from the bare gold layer; dashed curve shows the scattering from gold on top of which a thin Be layer has been evaporated.

to the beam were observed by electrostatic analysis. The face of the target was inclined at an angle of 45° with respect to the beam. Figure 1 shows a schematic of the experimental arrangement for target-thickness measurements. The target can be moved up and down to expose the desired portion to the collimated beam.

Owing to the high Z, the scattering from the thin layer of gold forms a pronounced peak. When the target is shifted so that the proton beam must pass through the beryllium layer to reach the gold, the peak is shifted towards lower energy corresponding to an energy loss in a distance $2t\sqrt{2}$ in the beryllium, of layer thickness t. The data for a typical target so studied is shown in Fig. 2. The shift shown here corresponds to a change of 0.81 kV in one plate of the analyzer, or 12.5-keV energy decrement in the beam. From the known stopping power of beryllium for protons, t for the layer is 9.9 $\mu g/cm^2$. A rough check was obtained by the scattering of a Li^6 ion beam of 3.3 MeV from the two portions of the target. Within the limits of energy resolution of the analyzer and a rough estimate of the stopping power for beryllium based on the measurements of Allison *et al.*,[8] the agreement was good. The method assumes, however, that the layer obtained by evaporation is actually metallic beryllium.

The apparatus for the measurement of the energy and angular distribution of the reaction products is essentially that described by Huberman *et al.*[9] and is shown in Fig. 3. The upper half of the reaction chamber is coupled to a proportional counter and a solid-state detector. The reaction products traverse the proportional counter at right angles to the axial anode wire producing a pulse proportional to the energy loss (ΔE).

[8] S. K. Allison, D. Auton, and R. A. Morrison, Phys. Rev. **138**, A688 (1965).

[9] M. H. Huberman, M. Kamegai, and G. C. Morrison, Phys. Rev. **129**, 791 (1963).

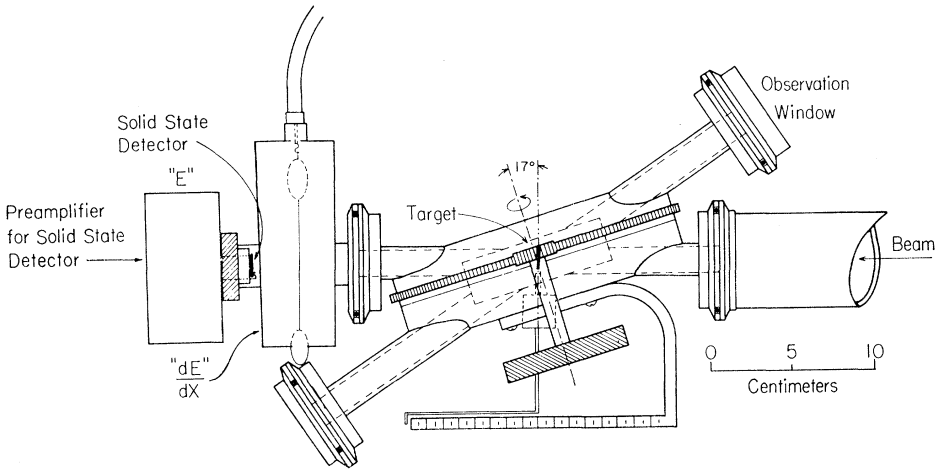

FIG. 3. Target chamber for the angular-distribution measurements.

The proportional counter uses methane gas and is a continuous flow type. The pressure is maintained at a fixed value by using a manostat. The target chamber is isolated from the proportional counter by the use of a very thin film supported on a wire gauze. This film was prepared by using "New Skin" manufactured by Newskin Company, Brooklyn, New York. A drop of this liquid on the surface of distilled water spreads to a uniform film which can be picked up by a suitable film holder. The average thickness of the films used in this work was 35 $\mu g/cm^2$, as determined by weighing. The particles are stopped by a solid state detector giving rise to an E pulse. These two pulses after suitable amplifications are brought to the vertical deflection plate (Y) and the horizontal deflection plate (X) of a fast cathode ray tube, respectively. The trace on the oscilloscope is intensified by providing a Z or intensifying signal whenever a coincidence occurs between the E and ΔE pulses. Particles of the same mass and charge but of different energy trace out approximately hyperbolic patterns on the screen. The patterns can be observed visually or photographed using a polaroid camera. Whenever particle discrimination is desired, a black masking tape can be used to cover the traces of all but the desired particles. A photomultiplier looks at the screen, giving a pulse whenever a light flash due to coincident E and ΔE pulses appears. This pulse is used after shaping properly to gate a 400 channel RIDL pulse height analyzer which responds to E pulses whenever the gate opens. A block diagram (Fig. 4) illustrates the main features of the setup. The arrows indicate the direction of propagation of the pulses. The polarities of the pulses at various stages are also indicated by + or − sign.

The solid state detector subtends a solid angle of 1.47×10^{-3} sr and is capable of furnishing a depletion depth of 200 μ suitable to stop alpha particles of about 20-MeV kinetic energy. The detector was calibrated using a Th C' α source. The two α peaks of 6.09 and 8.78 MeV were compared with two settings of an ORTEC precision pulse generator. Over a long period of time it was observed that these settings remained the same within 0.1%, even when the detectors were replaced by another of the same type. At the start of each run, the analyzer was calibrated by these two improvised alpha peaks. This was again checked at the end of each run. Electronic drifts were always negligibly small.

The beam was collimated to $\frac{1}{8}$ in. in diam before hitting the target. The plane of the target could be fixed in any desired position with respect to the beam. In all the experiments, the plane of the target was fixed at half the angle which the detector made with the beam direction.

The methane gas pressures used in the proportional counter in this experiment were normally 1 cm of Hg

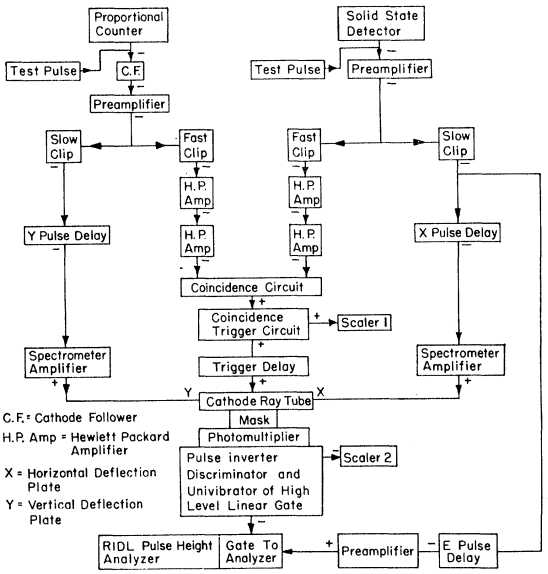

FIG. 4. Block diagram of the electronic circuits comprising the particle-selection system.

when Li^7 gated spectra were taken and 2 cm of Hg when α-gated spectra were observed. The path length for the charged particles in the proportional counter was 5.49 cm. Since for both these types of particles, the loss in energy in the methane at the pressures used is a very small fraction of the energy and the loss in 35-$\mu g/cm^2$ New Skin film is very small, the elastically scattered Li^6 ions of practically all energies could reach the detectors. The resulting electronic pile-up prevented us from studying angles below 30° and also confined our studies of charged particle spectra to energies above 3.0 MeV in the laboratory system.

In most of the product-particle counts made during these experiments the beam current collected by the target was used as a monitor. Part of the information needed to reduce the data to fundamental units is the number of projectile particles which have hit the target during the run. The following two difficulties are present in the reduction of total measured microcoulombs to numbers of Li^6 nuclei:

(a) The well-known difficulty due to the release of secondary electrons from the target and from the surfaces of the bombardment chamber which could see the target.

(b) The difficulty in knowing the effective charge per particle in the beam. Although the charge per projectile particle is known where the beam leaves the sorting magnet on its way to the target, it may capture or lose electrons along its path due to poor vacuum in the beam tube or scattering from aperture edges, etc.

In connection with item (a), a series of tests of the effect of secondary electrons were made, using positive-target biasing and a negatively biased screen near the boundaries of the target chamber to suppress secondaries from the walls. The arrangement was adjusted until it met the tests of invariance of measured current with variable bias over considerable ranges of bias voltage, and its invariance with angle between the target face and the beam. The screen was found necessary to maintain constant and positive current at small angles. The beam current was measured by allowing it to flow into a Plasticon capacitor with a 5000 V rating and sensing the voltage rise by a Cary vibrating-reed electrometer.

For item (b) above, tests of the effective charge of the beam were made by placing a 0.175 ± 0.01 mg/cm² gold foil over a thick beryllium backing and observing the Rutherford scattering of the Li^6 beam from the gold. The observations were made at $\theta_{lab}=90°$ and with the plane of the target making an angle of 45° with the incoming beam. The scattered Li^6 particles formed an intense group at the calculated energy, and about 400 keV in energy spread at half-maximum, which corresponds to a reasonable value (250×10^{-15} eV×cm²/atom) for the stopping of 3.3-MeV Li^6 particles in gold.

The target chamber was 198 cm from the exit port of the sorting magnet, at which port the beam charge was defined by the Van de Graaff energy and the magnetic field. The ratio of total number of scattered Li^6 particles to measured μC of beam impinging on the target was observed at 1.9 MeV Li^6 kinetic energy. With the magnet set to deflect Li^+, the pressure in the beam tube was varied from about 5×10^{-6} mm to 45×10^{-6} mm, which amply covered the range of pressures in which measurements were made (see Fig. 5). The scattered counts per μC of beam did not vary in this pressure interval, indicating that the effective beam charge did not change. Then with the magnet set to deflect Li^{++} of the same energy, the experiment was repeated and showed that the effective beam charge again was pressure-invariant, and since the observed counts per microcoulomb were half of those with the magnet set for Li^+, that the effective beam charge had doubled.

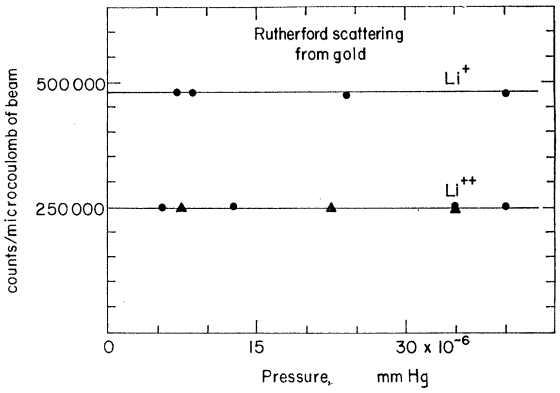

FIG. 5. Test of the effective charge of the lithium beam. Rutherford scattering of 1.9-MeV Li^6 from a 0.175 ± 0.01 mg/cm² gold film at a laboratory angle of 90°. Solid dots are for 1.9-MeV Li^6, whereas solid triangles represent data taken for 3.3-MeV Li^{++} normalized to the counts for 1.9-MeV Li^{++} at a pressure of 40×10^{-6} mm of Hg. Solid angle subtended by the detector is 1.47×10^{-4} sr.

Absolute determination of the beam charge using the Rutherford formula showed effective charges of one and two within 10–15%. The uncertainty arises partly from the uncertainty in the thickness and uniformity of the gold film. The ratio of the observed counts per microcoulomb of the Li^+ beam to the Li^{++} beam is, however, two within 4%. Tests with 3.3 MeV Li^{++} ions also showed invariance of effective charge with pressure. Thus, it may be safely concluded that the effective charge of the beam was not changed after it issued from the sorting magnet and before it impinged on the target.

Since in this experiment very thin films have been used to isolate the proportional counter from the target chamber, it becomes necessary to support these films on some wire gauze or screen. The transmission coefficient of this supporting screen was determined by microscope measurements and by counting the alpha particles from a ThC′ source with and without the supporting screen

in position. In a similar fashion, the transmission coefficient of the previously mentioned biasing screen was determined. The combined transmission coefficient with both screens in position was found to be 0.30. The observed spectra in the laboratory shown in this work have not been corrected for this transmission factor. All data analysis, however, takes into account this fact.

III. RESULTS

Hobbie *et al.*[10] (hereafter referred to as the Minnesota group) have studied the α groups of the reaction $Be^9(Li^6,\alpha)B^{11}$. They have made differential cross-section measurements on the alpha particles corresponding to the ground state and first seven excited states in B^{11}. They measured the absolute cross sections by comparison with Rutherford scattering which obviates the necessity of knowing target thickness or the solid angle. The thin targets, whose preparation has been described earlier, were used by us to repeat the above measurements. A typical α spectrum obtained at a laboratory angle θ_l of 90° is shown in Fig. 6. Vertical lines as indicated in the figure, are the calculated positions of the alpha peaks corresponding to the known excited states in B^{11} (taken from Ref. 6) and have been corrected for the energy loss in the New Skin film and the methane in the proportional counter. The spectrum was, however, obtained without making use of the particle-selection system, i.e., the analyzer was not gated. Since the intention was to compare our results with the results obtained by the Minnesota group, we used one of the two bombarding energies they had used in their experiment. We carried our measurements from 45° to 135° laboratory angles at intervals of 15°.

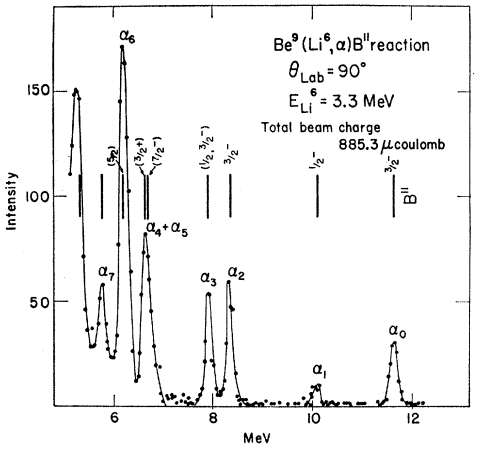

FIG. 6. Typical alpha spectrum from the $Be^9(Li^6,\alpha)B^{11}$ reaction for a thin target. The intensity represents the number of observed events. The intensity of α_2 is enhanced because of alpha particles from the Li^6+C^{12} reaction.

[10] Russell K. Hobbie, C. W. Lewis, and J. M. Blair, Phys. Rev. **124**, 1506 (1961); J. J. Leigh and J. M. Blair, *ibid.* **121**, 246 (1961).

Qualitative features of our work on the cross sections of some of the highest energy alpha groups agree well with the results of the Minnesota group. However, because of our observation that some alpha groups from Li^6+C^{12} and Li^6+O^{16} appear with intensities comparable to the alphas from Be^9, we have not made any quantitative estimates of absolute cross sections for fear the contamination may have occurred during target preparation and hence made the thickness measurements unreliable.

A gated alpha spectrum obtained with a thick target is shown in Fig. 7. This is also at 90° lab angle and with $E_{Li^6}=3.3$ MeV. A Mylar window of 0.15×10^{-3}-in. thickness was used in this instance to isolate the proportional counter from the reaction chamber. Alpha peaks corresponding to different excited states of B^{11} been appropriately labeled. The energies are uncorrected for losses in methane and Mylar. The spectrum can be compared with that in Fig. 6. The alpha particles of energy below about 2 MeV have been cut off due to the manner in which masking tape is pasted on the oscilloscope screen of the particle selection system. A series of such spectra at $\theta_l=90°$ were taken by varying the bombarding energy. The excitation function for the ground state alpha group is shown in Fig. 8. This has been taken at six bombarding energies from 3.0 to 3.75 MeV at intervals of 150 keV. A least-squares fit of the data gives a slope of 15.14 ± 0.65 particles/MeV μC of the incident beam.

The excitation curves for three other highest energy α groups were plotted and treated similarly to get the slope or the increase in yield per MeV per microcoulomb of the incident beam for use in Eq. (1).

The thick-target formula for the differential cross section is written as

$$d\sigma/d\Omega=(\epsilon/N_pN_t)/(dY/dE)1/\Omega, \qquad (1)$$

in which N_p is the number of Li^6 nuclei per microcoulomb of beam; N_t is the number of Be^9 nuclei per milligram of target material; dY/dE is the slope of the yield curve in units of number of particles produced per MeV energy interval per microcoulomb of incident beam; ϵ is the stopping power of the target material for Li^6 particles of the beam energy, expressed in MeV per milligram per cm^2, and is considered a positive quantity; and Ω is solid angle subtended by the detector.

ϵ was estimated from the stopping power of beryllium for protons of the same velocity, as read from the data collected by Whaling.[11] The stopping power ϵ of a medium for a heavy ion beam of nuclear charge Z, divided by its stopping power ϵ_H for a proton of the same velocity is connected with the average beam charge by

$$\left.\frac{\epsilon}{\epsilon_H}\right|_V=\sum_{i=1}^{Z} i^2F_{i\infty}, \qquad (2)$$

[11] Ward Whaling, in *Handbuch der Physik*, edited by S. Flügge (Springer-Verlag, Berlin, 1958), Vol. 34.

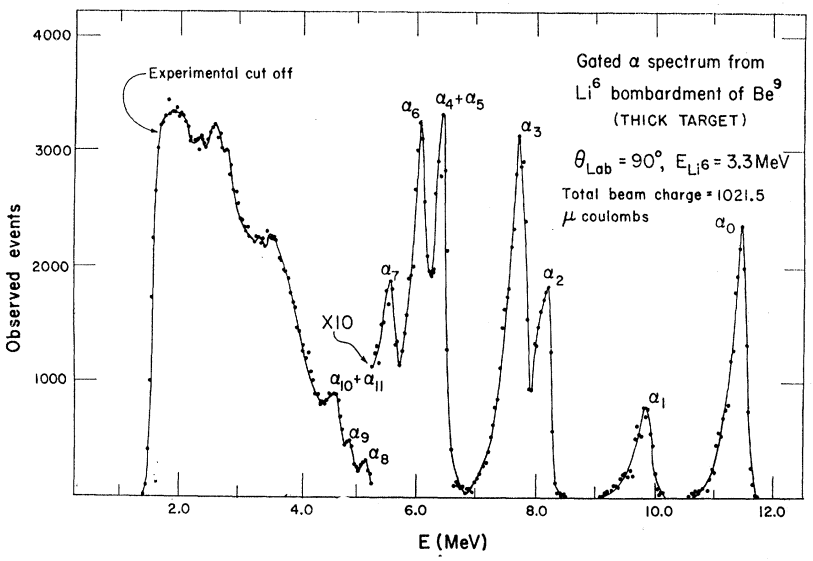

FIG. 7. Typical alpha spectrum in the laboratory system from a thick target of beryllium.

where $F_{i\infty}$ is the fraction of the ions of positive charge $i|e|$ in the beam. From stopping powers measured in other substances this sum was estimated to be 7.8 (see Fig. 2 of Ref. 8) for 3.3-MeV Li^6 ions in beryllium. This leads to a stopping power of 2.55 MeV×cm²/mg. This value has been used in all the data analysis.

The differential cross sections for the four highest energy α groups from the $Be^9(Li^6,\alpha)B^{11}$ reaction corresponding to B^{11} being left in the ground state, first excited state, second excited state and third excited state are shown in Fig. 9. The data are for a thick target. The errors shown are statistical and also combine the error in the least-squares fit of the slope dY/dE of the excitation curve of the pertinent α group. The general features of these angular distributions are in very good agreement with the Minnesota work.[10] However, the absolute cross sections are very roughly half of their values. A very careful check of all the parameters involved in the calculation of the cross sections has been made without revealing the cause of this discrepancy. The Minnesota work has involved the use of the Rutherford scattering formula. Bennett

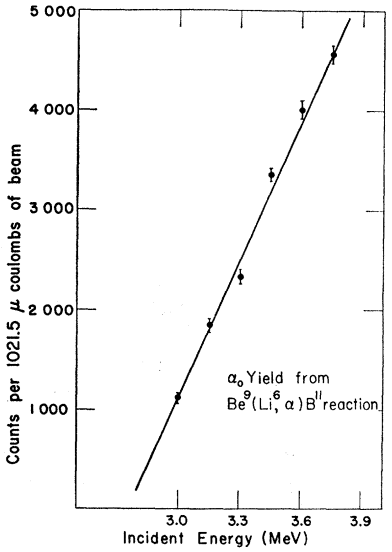

FIG. 8. Thick target yield of α_0 from the $Be^9(Li^6,\alpha_0)B^{11}$ reaction as a function of bombarding energy.

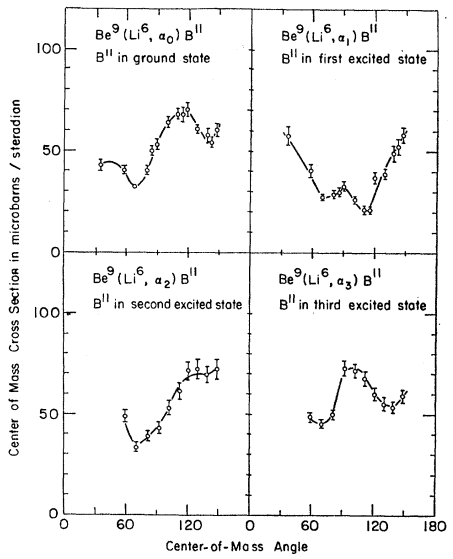

FIG. 9. Differential cross sections for the four highest energy alpha groups from the $Be^9(Li^6,\alpha)B^{11}$ reaction.

and Grant[12] have studied the elastic scattering of Li^7 ions of 7.3-MeV energy from C^{12}. In this work the apsidal distance of the Rutherford orbit is about $\frac{2}{3}$ of that of the Minnesota experiment for the same angular range (lab angles 30°–50°). Bennett and Grant, however, find the $\sigma_{obs}/\sigma_{Rutherford}$ to be lower than 0.5 in the angular range studied by the Minnesota group. Although the Minnesota group checked within experimental errors the constancy of the ratio of the yield $Y(\theta)$ to the Rutherford scattering cross section $\sigma_R(\theta)$ with angle in the range of θ_l from 30° to 50°, it is possible that absolute values of the observed cross section may be lower than the theoretically calculated value. This might explain the discrepancy between the values obtained by them and in the present work.

Li^7 Spectrum

Figure 10 shows a typical gated spectrum of Li^7 obtained at 40° in the laboratory by using a thick target at $E_{Li^6}=3.3$ MeV. Since the particle selection system is incapable of distinguishing between Li^6 and Li^7, the lower energy part of the spectrum has elastically scattered Li^6 superposed on it, although the latter was partially masked off on the oscilloscope screen of the particle selection system. The lower energy cutoff for the useful spectrum was estimated by assuming that iron is the heaviest element occuring as impurity in the beryllium of the target. By rejecting the spectrum below this energy we could be reasonably sure that no elastically scattered Li^6 would interfere in the spectrum analysis.

The spectrum apparently extends somewhat beyond the kinematically possible energy limit and, in general, the same feature has been observed for other Li gated

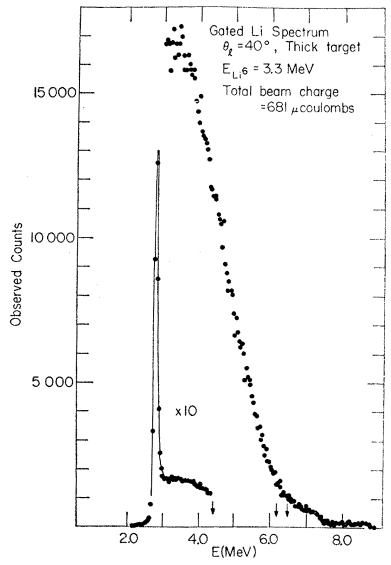

FIG. 10. A typical gated Li^7 spectrum as observed in the laboratory from the Li^6+Be^9 reaction; energies have been corrected for losses in the window and gas of the proportional counter.

[12] J. R. J. Bennett and I. S. Grant, *Reactions Between Complex Nuclei* (University of California Press, Berkeley, 1963), p. 50.

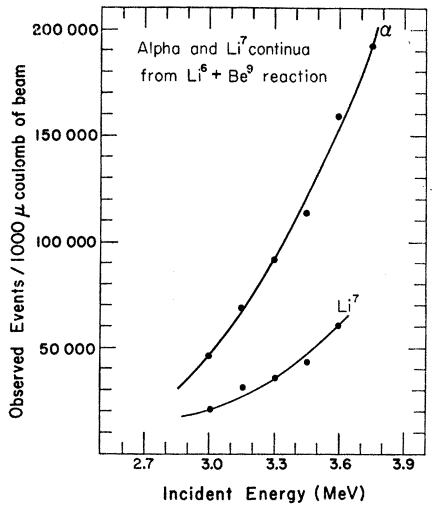

FIG. 11. Yield of Li^7 and α particles under the continua as a function of the bombarding energy. Li^7 continuum above $E_{Li^7}=3.5$ MeV and the α continuum above $E_\alpha=2.86$ MeV only were analyzed. Curves are appropriately labeled.

spectra. The reasons are, perhaps, not difficult to comprehend. Proportional counters are known to give rather poor energy resolutions. In the present experiment, the proportional counter has been used for the measurement of the energy lost within its sensitive region by various charged particles. The pulse-height distributions, however, are broad enough so that there is some overlap between the pulse distributions from Li and He ions. The masking procedure to eliminate gate pulses created by alpha particles will still allow some to appear above the masked region and be counted as Li pulses and vice versa.

Spurious gate pulses can also arise from pile-up of pulses at high counting rates. Since elastically scattered Li^6 ions contribute the highest counting rate, they form the most likely source of these pulses. However, thees pulses can only add to one another, or to some other pulses. This would tend to make them lie higher than the Li^6 pattern (adding up of ΔE pulses) and/or to the right of the Li^6 pattern (adding up of E pulses) on the screen. No significant contribution from this effect was observed in the photographs of the screen, and in any case the masking was placed so as to eliminate most of it. The remainder would be counted in the extension of the spectrum beyond the kinematic limit. From these considerations, we estimate an upper limit of 10% of the counts under the continuum to be due to these effects.

The spectrum shows no evidence of a discrete energy peak as would be expected if the reaction proceeded as a two-body reaction, i.e., $Be^9(Li^6,Li^7)Be^8$. The arrows read from right to left, correspond to the expected location of discrete energy peaks in the spectrum corresponding to (1) the ground states of both Li^7 and Be^8; (2) Li^7 in first excited state and Be^8 in its ground

state; and (3) Be^8 in first excited state, whereas Li^7 is in its ground state.

In order to obtain the excitation function of the continuum such spectra were taken at $\theta_l=60°$ as the bombarding energy was raised from 3.0 to 3.60 MeV. Figure 11 shows a curve showing the yield of Li^7 ions in the continuum with energies above 3.5 MeV. The energies have been corrected for loss in methane and in the New Skin film. By rejecting data below 3.5 MeV, no contribution could come from Rutherford scattering of Li^6 ions from impurities in the beryllium, even at the highest bombarding energies. The curve gives a slope dY/dE at 3.3 MeV bombarding energy equal to 192 counts/MeV μC for $\theta_l=60°$. To obtain a value of dY/dE at 3.3-MeV incident energy at other laboratory angles, the yield under the continuum for 3.3-MeV bombarding energy at these angles was compared with the yield under the continuum at 60° lab at the same bombarding energy and normalized to the same total beam charge. The ratio so obtained, multiplied by dY/dE at $\theta_l=60°$ was taken as the dY/dE at the other angle.

Alpha Continuum

By subtracting the discrete energy peaks from the alpha spectrum observed in the laboratory such as shown in Fig. 7, the yield Y under the continuum was obtained. A lower cutoff of about 2.0 MeV because of greater energy loss in the Mylar window and gas was sufficient to ensure against any contribution coming from elastically scattered Li^6 ions, as the latter produce very bright spots on the screen of the particle selection system. A series of such spectra were taken at $\theta_l=90°$ by varying the bombarding energy from 3.0 to 3.75 MeV in steps of 150 keV. Figure 11 shows the yield Y under the continuum plotted as a function of E_{Li^6} at $\theta_l=90°$. The lower cutoff for the energy spectrum used in the data analysis after correcting for the losses in 0.00015-inch Mylar window and the methane gas of the proportional counter is about 2.86 MeV. The slope of the curve at $E_{Li^6}=3.3$ MeV gives a value of 587 particles/MeV μC for dY/dE. In order to make an estimate of dY/dE at other laboratory angles, the yield under the continuum at those angles was compared with the yield under the continuum at $\theta_l=90°$ for the same bombarding energy (3.3 MeV) and normalized to the same amount of total beam charge striking the target.

Differential Cross Sections and Transformation to the Center-of-Mass System

In the case of continuous spectra, the results are usually expressed in terms of the quantity $d^2\sigma/d\Omega dE$, the differential cross section in cm²/sr MeV. It can be easily seen that for a thick target $d^2\sigma/d\Omega dE$ at a laboratory energy E is given by

$$\frac{d^2\sigma}{d\Omega dE}=\frac{N_{\text{obs}}}{\Delta E\sum N_{\text{obs}}}\frac{\epsilon}{N_pN_t}\frac{dY}{dE}\frac{1}{\Omega}. \tag{3}$$

N_{obs} = number of events observed in energy interval ΔE at energy E; $\sum N_{\text{obs}}$ = total number of counts observed under the continuum. Other quantities are defined the same way as in Eq. (1). However, Y here is the yield under the whole continuum observed.

The transformation to the center of mass is carried out as follows:

If E_c is the kinetic energy, θ_c and ϕ_c are the polar and the azimuthal angles in the center of mass system and E_l, θ_l, ϕ_l are the corresponding quantities in the laboratory system, one can write

$$\frac{d^2\sigma(E_c,\theta_c,\phi_c)}{dE_cd\Omega_c}=J\left(\frac{E_c,\theta_c,\phi_c}{E_l,\theta_l,\phi_l}\right)\frac{d^2\sigma(E_l,\theta_l,\phi_l)}{dE_ld\Omega_l}, \tag{4}$$

where J is the Jacobian determinant.

If one is not dealing with either polarized beams or polarized targets, J is simply

$$J\left(\frac{E_c,\theta_c}{E_l,\theta_l}\right).$$

This expression can be easily calculated from geometric considerations[13] and is included in the general statement that $p^{-1}(d\sigma^2/d\Omega dE)$ is invariant,[14] where p is the momentum. At nonrelativistic energies, the Jacobian will thus be given by

$$J\left(\frac{E_c,\theta_c}{E_l,\theta_l}\right)=\frac{V_c}{V_l}. \tag{5}$$

From Fig. 12, simple geometric considerations give

$$V_c^2=V_l^2+V_{cl}^2-2V_lV_{cl}\cos\theta_l; \tag{6}$$

V_{cl} is determined by projectile energy. V_l and θ_l can be uniquely fixed for a given θ_c and V_c by the relations:

$$V_l^2=V_c^2+V_{cl}^2+2V_cV_{cl}\cos\theta_c, \tag{7}$$

$$\sin\theta_l=(V_c/V_l)\sin\theta_c=\sin\theta_c[1+(V_{cl}/V_c)^2+(2V_{cl}/V_c)\cos\theta_c]^{-1/2} \tag{8}$$

and thus, expressed in terms of V_l and θ_l

$$J=(V_c/V_l)=[1+(V_{cl}/V_l)^2-2(V_{cl}/V_l)\cos\theta_l]^{1/2}. \tag{9}$$

To obtain $d^2\sigma(E_c,\theta_c)/d\Omega_cdE_c$ from the experimental data, one plots the observed $d^2\sigma(E_l,\theta_l)/d\Omega_ldE_l$ versus E_l for a given θ_l. To deduce the barycentric energy profile (variable E_c) at fixed θ_c, it is necessary to calculate for each (E_c,θ_c), the corresponding E_l and θ_l

[13] S. K. Allison, Nucl. Phys. (to be published).
[14] A. H. Rosenfeld, Phys. Rev. **96**, 130 (1954).

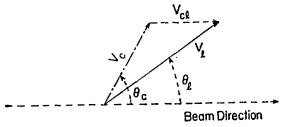

FIG. 12. Vector diagram for the transformation of a particle velocity V_c in the barycentric system to its velocity V_l as it appears in the laboratory system, in which system the velocity of the barycentric system is V_{cl}.

using the relations Eqs. (7) and (8). From the above series of curves, one reads off the values of $d^2\sigma(E_l,\theta_l)/d\Omega_l dE_l$ at the calculated value of E_l from the two curves, between which the calculated value of θ_l lies. Thus, by interpolation, one gets $d^2\sigma(E_l,\theta_l)/d\Omega_l dE_l$ for a given E_c and θ_c and multiplies the value so obtained by the pertinent value of the Jacobian to get $d^2\sigma(E_c,\theta_c)/d\Omega_c dE_c$.

The procedure outlined above was followed to plot curves showing $d^2\sigma/d\Omega_c dE_c$ versus E_c for the case of alpha continuum as well as the Li^7 continuum and are shown in Figs. 13 and 14. The data were taken with a thick target and at a bombarding energy of 3.3 MeV.

Total Cross Sections

The total cross section σ_t can be obtained from the differential cross section by

$$\sigma_t = 2\pi \int_{-1}^{+1} \left[\int_{E_{\min}}^{E_{\max}} \frac{d^2\sigma}{d\Omega dE} dE \right] d(\cos\theta). \quad (10)$$

In the present work because of the difficulties associated with distinguishing between Li^7 and elastically scattered Li^6, $E_{\min}$ of the data analyzed could not be zero for the Li^7 spectrum but a finite value (3.0 MeV) in the laboratory system. When the laboratory spectra observed above 3.0 MeV in the course of this work are transformed into the center of mass system, Li^7 kinetic energies down to 1.4 MeV in the center of mass system for $\theta_c = 50°$ can be observed. For larger θ_c, the corresponding lower energy limit is higher; for 110°; the largest reliable θ_c resulting from the transformation, the lower limit was 3.4 MeV. From Fig. 14 the spread of these points shows that within experimental errors, the differential cross sections $d^2\sigma/d\Omega dE$ are independent of θ_c or, in other words, the distribution of Li^7 particles is isotropic in the center of mass system. The spectral distribution of Li^7's appears to extend beyond the kinematic limit. The probable cause has been explained in the discussion of Li^7 spectrum observed in the laboratory. If we integrate the area under this curve, from 1.4 MeV to the end point which is very nearly 4.15 MeV, we get

$$\int_{1.4\text{ MeV}}^{4.15\text{ MeV}} \frac{d^2\sigma}{d\Omega dE} dE = 1.16 \pm 0.12 \text{ mb/sr}. \quad (11)$$

On the assumption that the distribution is isotropic in the center of mass system, this would correspond to

$$\sigma_t(E_c > 1.4 \text{ MeV}) = 14.6 \pm 1.5 \text{ mb}. \quad (12)$$

The curve has been extrapolated to zero energy taking into account the volume in phase space available to the three particles. The distribution function $f(E_3)$ for a three-body breakup is given by[15]

$$f(E_3)dE_3 \propto E_3 \left(E - \frac{m_1+m_2+m_3}{m_1+m_2} E_3 \right)^{1/2} dE_3, \quad (13)$$

where E_3 is the barycentric energy of particle 3, E is the total energy available in the center-of-mass system and the m's are the respective masses of the three particles. The expression, however, does not take into account the effect of the Coulomb force or any other final state interaction as there is no simple way to introduce these effects. The function $f(E_3)$ is plotted in Fig. 15 for both Li^7 and α particles. In the extrapolation, the assumption has been made that the maximum possible error in the extrapolated area cannot exceed the shaded area which is $\frac{1}{2}$ the area projected to the left of the actually observed data. Any reasonable extrapolation of the observed curve, bearing in mind the phase space considerations, will not give a cross section higher or lower than the indicated limits. This gives

$$\int_0^{4.15\text{ MeV}} \frac{d^2\sigma}{d\Omega dE} dE = 1.93 \pm 0.61 \text{ mb/sr} \quad (14)$$

at 3.3-MeV laboratory bombarding energy, corresponding to a total cross section

$$\sigma_t = 24.3 \pm 7.7 \text{ mb} \quad (15)$$

on the assumption of isotropic distribution. This may be compared to the total cross-section of $Be^9(Li^7,Li^8)Be^8$ reaction at 3.3-MeV bombarding energy equal to 43.3 mb as observed by Norbeck *et al.*[2]

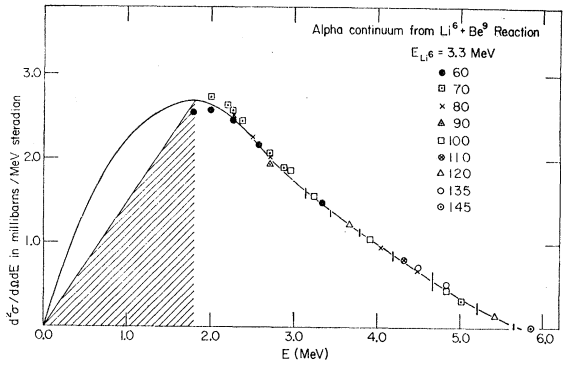

FIG. 13. Barycentric energy profile of the alpha continuum from the Li^6+Be^9 reaction. Vertical lines at certain energies are drawn to show the total spread of $d^2\sigma/d\Omega dE$ for all angles for which the laboratory data are available.

[15] G. E. Uhlenbeck and S. Goudsmit, *Verhandelingen van Dr. P. Zeeman* (Martinus Nijhoff, The Hague, 1935), p. 201.

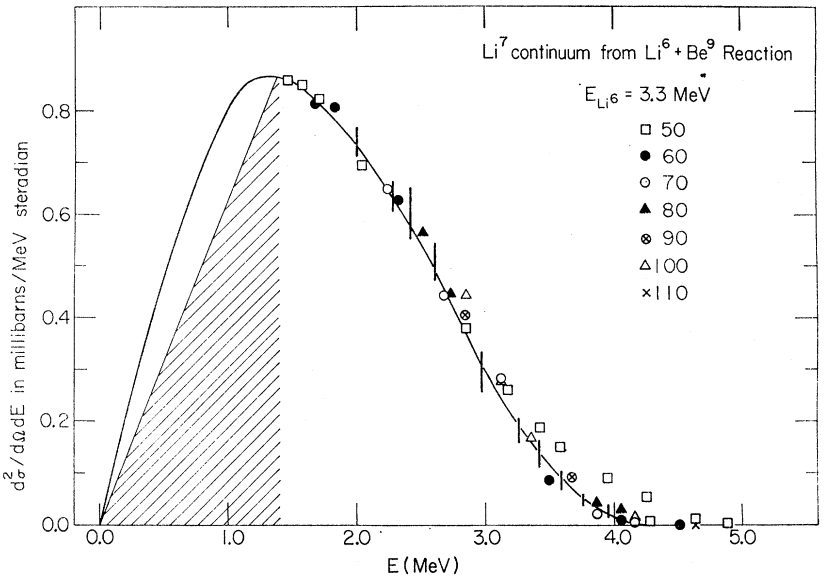

FIG. 14. Barycentric spectral distribution of Li^7 particles from the Li^6+Be^9 reaction. See caption for Fig. 13.

In much the same way, the α-continuum data have been treated as shown in Fig. 13. In the center-of-mass system the data at angles from 60° to 145° have been plotted corresponding to the laboratory data from 40° to 140°. Here again the barycentric distribution seems to be isotropic within experimental errors. The lower energy cutoff in this case extends down to 1.8 MeV, and to obtain an estimate of the total cross section for α continua, an extrapolation similar to that for the Li^7 continuum has been made. Table II summarizes the results deduced from the area under the curves.

TABLE II. α continuum from Li^6+Be^9 at $E_{Li^6}=3.3$ MeV.

Energy region	$\int \frac{d^2\sigma}{d\Omega dE} dE$ at any θ_c in mb/sr	σ_t [cf. Eq. (10)] in mb
1.8 MeV → end point	4.89±0.49	61.5±6.2
3.81 MeV → end point	1.00±0.10	12.6±1.3
0.0 MeV → end point	8.21±2.4[a]	103.2±30.3[a]

[a] This error is the error discussed in the text.

IV. DISCUSSION

The Reaction Mechanism and the α Groups

The Coulomb barrier for the Li^6+Be^9 reaction is $(4.434/r_0)$ MeV or 2.95 MeV for an $r_0=1.5$ F. The energy available in the center-of-mass system at 3.3-MeV bombarding energy is only 1.98 MeV, which is below the barrier height. The distance of closest approach in a head-on collision is 8.73 F. The probability of the formation of a compound nucleus at such low bombarding energy is thus small. The contention is supported by the absence of any resonances in the excitation functions which are smoothly rising functions of bombarding energies in this energy region. The compound nucleus, if formed, would be a very highly excited state at about 27 MeV in N^{15}. Carlson and Throop[16] have shown by observations of the high-energy gamma rays from the Li^6+Be^9 reaction that the upper limit of the cross-section for the formation of a compound nucleus with subsequent gamma de-excitation at 3.3-MeV bombarding energy is 1.4×10^{-30} cm². Leigh and Blair[10] have pointed out that at such highly excited states of the compound nucleus, the statistical model would be applicable for the angular distribution of the particles emitted giving a symmetric angular distribution around 90° in the center-of-mass system. The observations of the Minnesota group[10] and ours on the discrete alpha groups fail to show such a pattern.

Li^6 has been discussed as a cluster of $(\alpha+d)$ by many authors. It is highly probable that Li^6 which comes as

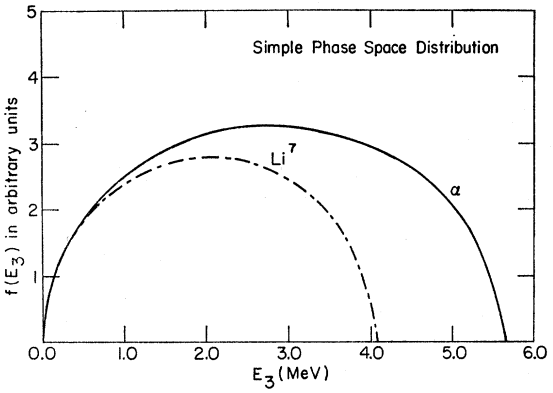

FIG. 15. Theoretical phase space distribution of the alpha particles and Li^7 particles versus energy in a simultaneous three-body breakup from the reaction $Li^6+Be^9 \rightarrow Li^7+2\alpha$.

[16] R. R. Carlson and M. Throop, Phys. Rev. **136**, B630 (1964).

close as 8.73 F to the Be^9 nucleus in a head-on collision (sum of the two radii ~5.6 F) transfers a deuteron to the latter. This is referred to as the normal or the projectile stripping. Another stripping mode called target stripping (or heavy particle stripping) is also considered as an additional mode of the reaction mechanism. In this picture, Be^9 is considered to be in a two-cluster configuration (α+He^5) at the time of interaction with the projectile Li^6. The latter picks up the He^5 cluster forming B^{11} and the α is emitted. The main difference is that whereas there is forward peaking in the former stripping mode, there is backward peaking in the heavy-particle-stripping mode. These stripping-theory pictures of the $Be^9(Li^6,\alpha)B^{11}$ reaction have been discussed by Leigh,[17] Rustgi,[18] and el Nadi and Sherif[19] with a fair amount of success.

The Li^7 Continuum and the He^4 Continua

Of the three possible reaction channels through which the Li^6+Be^9 reaction can proceed producing Li^7 (see Table I) only the $Be^9(Li^6,Li^7)Be^8$ reaction would give rise to discrete kinetic energies for Li^7 particles. The Q value of this reaction and the energy available in the center of mass from the bombarding energy, allows the populating of both the ground state ($J=0^+$, $T=0$) and the 2.90-MeV first excited state ($J=2^+$, $T=0$). The latter has a level width[6] Γ of 1.46±0.05 MeV, and if this state is also produced, the Li^7 kinetic energy spectrum will show a hump in addition to a sharp peak corresponding to the production of the Be^8 ground state. As an example of the type of spectrum which one would expect in this case, we refer to the reactions $B^{11}(p,\alpha)Be^8$ and $B^{10}(d,\alpha)Be^8$. In these reactions,[20] the alpha-particle spectra clearly exhibit the features mentioned above. However, the Li^7 spectra observed in the course of this work show no evidence of this nature. The spectra above 3.0-MeV kinetic energy for Li^7 are monotonically falling curves. This result is rather surprising in view of the fact that a simple neutron pickup by Li^6 from Be^9 which has a rather loosely bound neutron (binding energy 1.67 MeV) to the Be^8 core would be an obvious and simple model of the reaction mechanism producing Li^7, particularly so, in view of the fact that some of the features of the $Be^9(Li^7,Li^8)Be^8$ reaction can be easily explained within the framework of this picture. One should, however, note that no observations have been made on the kinetic energy spectrum of either Li^8 or Be^8 (or alpha particles therefrom) in the latter reaction. Only the angular distribution of Li^8 irrespective of its energy has been observed. The explanation on the basis of a simple neutron transfer could be fortuitous.

Lemeille, Marquez, and Saunier[21] (hereafter referred to as the Saclay group) measured the charged particles from Li^6+Be^9 which were counted in coincidence with the 0.479-MeV gamma ray from the de-excitation of Li^7. They suggest the following interpretation of the reactions producing associated continua of Li^7 and alphas.

$$Li^6+Be^9 \rightarrow \alpha_1+B^{11*},$$
$$B^{11*} \rightarrow \alpha_2+Li^{7*},$$
$$Li^{7*} \rightarrow Li^7+\gamma.$$

The superscript * refers to the 13.16-MeV excited state in B^{11} and the 0.479-MeV excited state in Li^7. Subscripts 1 and 2 refer to the first α (discrete energy) and the second α (continuous energy).

From the tables compiled by Ajzenberg-Selove and Lauritsen in Ref. 6, B^{11} levels above and including 8.923 MeV (with few exceptions) can de-excite by the emission of alpha particles. Using the * as superscript for B^{11} in any excited state, it is to be noted that B^{11*} when produced as a concomitant nucleus in the Li^6+$Be^9 \rightarrow \alpha_1$+$B^{11*}$ reaction (subscript 1 refers to α of discrete energy) is moving in the center of mass system. Its dissociation while moving will give rise to a continuum in the energy spectrum of alpha of Li^7 particles. Table III gives the maximum and minimum kinetic energies for alpha particles and Li^7 when produced as a result of the de-excitation of B^{11} in any of the above-mentioned highly excited states. The table also gives the corresponding maximum and minimum kinetic energies when the de-excitation occurs through the first excited state of I i^7 as suggested by the Saclay group for the 13.16-MeV level in B^{11}. The data used for the calculations is from Ref. 6. On the basis of the mechanism suggested by the Saclay group, at the bombarding energy used in the present work the E_{Li^7}(max) should be 3.77 MeV and E_α(max) should be 4.636 MeV. From

TABLE III. Center-of-mass energies for alphas and Li^7 when produced by de-excitation of B^{11} excited states. E_{Li^6}=3.3 MeV.

B^{11} level	When Li^7 is produced in ground state				When Li^7 is produced in first excited state			
	E_α		E_{Li^7}		E_α		$E_{Li^{7*}}$	
	Max	Min	Max	Min	Max	Min	Max	Min
8.923	1.567	0.196	2.037	0.666				
9.187	1.982	0.066	2.361	0.444	0.995	0.444	1.504	0.953
9.276	2.102	0.041	2.450	0.389	1.247	0.288	1.725	0.767
9.87	2.778	0.007	2.920	0.149	2.164	0.012	2.437	0.285
10.26	3.148	0.058	3.155	0.065	2.592	0.006	2.729	0.143
10.61	3.448	0.136	3.334	0.021	2.926	0.049	2.942	0.065
11.00	3.754	0.251	3.505	0.001	3.260	0.136	3.142	0.017
11.46	4.083	0.419	3.674	0.010	3.615	0.278	3.336	0.000
11.68	4.229	0.510	3.744	0.025	3.771	0.360	3.416	0.005
11.94	4.393	0.627	3.818	0.052	3.946	0.465	3.501	0.021
13.16	5.043	1.294	4.045	0.296	4.636	1.092	3.769	0.225
14.00	5.372	1.872	4.083	0.583	4.988	1.647	3.829	0.489
15.10	5.611	2.820	3.941	1.150	5.254	2.568	3.715	1.029

[17] J. J. Leigh, Phys. Rev. **123**, 2145 (1961).
[18] M. L. Rustgi, Nucl. Phys. **27**, 58 (1961).
[19] M. el Nadi and H. Sherif, Nucl. Phys. **28**, 331 (1961).
[20] R. E. Holland, D. R. Inglis, R. E. Malm, and F. P. Mooring, Phys. Rev. **99**, 92 (1955).
[21] C. Lemeille, L. Marquez, and N. Saunier, J. Phys. Radium (Paris) **22**, 586 (1961); M. Coste, C. Lemeille, L. Marquez and N. Saunier, *ibid.* **22**, 349 (1961); R. Ballini and N. Saunier, *ibid.* **24**, 904 (1963).

Figs. 13 and 14, it is obvious that this cannot explain all our results, as the maximum energy in the Li^7 continuum is 4.15±0.10 MeV, and in the α continuum 5.70±0.10 MeV in the center-of-mass system. This may be compared with the values expected for the simultaneous three-body breakup $Li^6+Be^9 \rightarrow Li^7+2\alpha$ which which gives $E_{Li^7}(\max)=4.083$ MeV and $E_\alpha(\max)=5.619$ MeV. The shape of the spectrum is also quite different from that suggested by the Saclay group except that the distribution is isotropic in the center of mass as predicted.

The excitation of B^{11} levels above 8.66 MeV at the bombarding energies used in the present experiment is entirely possible. No data, however, exist on the cross section for the excitation of these levels in the Be^9+Li^6 reaction. The present work also could not lead to any quantitative measurements of the cross section for the emission of alpha particles corresponding to these levels. However, quite a few of them are observed in the gated alpha spectrum. The large α-continuum background and the poor resolution due to the use of a thick target does not allow anything but a qualitative look at the alpha particles corresponding to these higher excited states in B^{11}. The Li^7 continuum, thus, should have a contribution from these levels. Carlson and Throop[16] have not observed any gamma-ray peaks above 9.0 MeV from the Li^6+Be^9 reaction which lends support to the above observation, since these levels may de-excite by particle emission, the latter being highly favored over electromagnetic transitions.

If we compare the results on the Li^7 continuum and the alpha continuum, we see that, as against a total cross section of 24.3±7.7 mb for the former, the cross section for the latter is 103±30 mb. The reason for this difference lies in the fact that in addition to the alpha particles associated with the Li^7 particles, there are four other α-producing reactions energetically possible (see Table I). Table IV gives the kinematics of these

TABLE IV. Non-Li^7-producing reactions which produce an alpha continuum. $E_{Li^6}=3.3$ MeV.

Reaction	Q (MeV)	Total energy available in center-of-mass system (MeV)	E_α (max) in the center-of-mass system (MeV)
$Be^9+Li^6 \rightarrow 3\alpha+t$	3.215	5.194	3.810
$\rightarrow \alpha+n+B^{10}$	2.891	4.870	3.573
$\rightarrow \alpha+p+Be^{10}$	3.118	5.098	3.739
$\rightarrow \alpha+t+Be^8$	3.121	5.100	3.741

four reactions in the barycentric system. We see from this table that none of these reactions can give any contribution to the α-continuum cross section above the barycentric $E_\alpha=3.81$ MeV. The σ_t for producing alpha particles of energy higher than 3.81 MeV in the center-of-mass system is 12.5±1.3 mb. Comparing this with the value of $\sigma_t=24.3\pm7.7$ mb for the production of Li^7 continuum of all energies, we realize the following:

1. The only two methods of producing alpha particles with continuous kinetic energy distribution above 3.81 MeV in the center-of-mass system are (a) the 3-body breakup $Li^6+Be^9 \rightarrow Li^7+2\alpha$; and (b) de-excitation of B^{11} excited states at 11.46 MeV and higher.

2. If 1(b) is the only mechanism, plus the contribution from other excited states of B^{11} mentioned in Table III, there is one alpha particle in the continuum for each Li^7 particle in the continuum. The difference of the two cross sections (24.3∼7.7)−(12.5±1.3) would have to be contributed by alphas of energies lying between 0.006 and 3.81 MeV. Such a distribution would tend to have a maximum around 3.8 MeV since about 12 mb will have to be contributed by the area under the curve extending from 3.8 down to 0.006 MeV. Phase space considerations will not justify such a distribution, which will have to contribute about the same area for the energy interval 0.006 to 3.81 MeV as the area under the continuum from 3.81 MeV to the end point.

3. Three-body breakup, i.e., 1(a), however, requires the production of two alpha particles for each Li^7 particle produced. In other words, the cross-section for the production of alpha continuum would be twice as large as that for Li^7. A more reasonable extrapolation of the $d^2\sigma/d\Omega dE$ curves for the α continuum at energies below 3.81 MeV can be done in this case. However, this cannot be the only mechanism involved, since alpha particles corresponding to the excitation of the B^{11} levels mentioned are observed. These considerations suggest that both of these mechanisms are responsible for the production of the continua of Li^7 particles and the alpha particles.

The observation that the Li^7 continuum has no evidence for discrete energy peaks is extremely puzzling. As mentioned earlier, the neutron in Be^9 is known to be loosely bound to the Be^8 core. For a square-well potential of 3 F radius, the neutron[22] has a 56% probability of being outside the well and 24% of being outside of 5 F. Li^6 can thus pick up this neutron at quite large radii to form Li^7. The absence of groups of Li^7 particles of discrete energy, however, implies that the core must break up simultaneously into two alpha particles, but it is not clear why such a picture does not explain the reactions initiated by lighter particles. In the case of lighter projectiles such as H^1 and H^2 the Coulomb barrier is only ∼1 MeV and broad resonances are observed in the reactions which correspond to the pickup of a neutron, suggesting the formation of a compound nucleus. The $Be^9(He^3,He^4)$ reaction below the Coulomb barrier is of interest in this connection. Bigham[23] has studied this reaction at $E_{He^3}=0.90$ MeV. The spectrum shows a weak ground-state group and a

[22] F. H. Read and J. M. Calvert, Proc. Phys. Soc. **77**, 65 (1961).
[23] C. B. Bigham, quoted by D. A. Bromley and E. Almqvist, Repts. Progr. Phys. **23**, 544 (1960).

broad group corresponding to the 2.90-MeV state in Be^8 superposed on the alpha continuum. The intensity of the group corresponding to the 2.9-MeV state in Be^8 is 20 times that of the ground state group in the spectrum observed at $\theta_l=90°$. The alpha continuum is quite prominent indicating that the neutron pickup by He^3 may also lead to a simultaneous breakup into three alphas.

The simultaneous breakup of the Be^8 core can also be visualized in the following manner.[24] When picking up a neutron, Li^6 comes so close to the Be^8 core that the Coulomb repulsion between Li^6 and the Be^8 core becomes strong enough so that Be^8 is effectively excited to a very highly excited state, i.e., it breaks up into two α particles. The large Coulomb repulsion must affect the Be^8 core. It is possible that the first excited state in Be^8 is also formed. Since so many highly excited states in B^{11} contribute Li^7 particles to the continuum, it might be possible for the latter to mask the Li^7 group corresponding to the broad first excited state of Be^8.

[24] F. C. Khanna (private communication).

ACKNOWLEDGMENTS

The author wishes to express his gratitude to Professor S. K. Allison for his sponsorship and guidance throughout this work. The assistance given by John Erwood, Walter Edwards, and Larry Palmer in operating the Van de Graaff and maintenance of the equipment are gratefully acknowledged. Walter Tomasek built a great deal of the equipment which facilitated this experiment. Dr. John Honsaker provided many helpful suggestions and stimulating discussions. Thanks are due to Dr. David Inglis and Dr. George Morrison of the Argonne National Laboratory for discussions which greatly aided the interpretation of the results of this work.

PHYSICAL REVIEW VOLUME 142, NUMBER 3 FEBRUARY 1966

$Ca^{46}(d,p)Ca^{47}$ Reaction at 7-MeV Bombarding Energy*

T. A. Belote, H. Y. Chen, and Ole Hansen†
Department of Physics and Laboratory for Nuclear Science, Massachusetts Institute of Technology, Cambridge, Massachusetts
AND
J. Rapaport‡
Departamento de Fisica, Universidad de Chile, Santiago, Chile
(Received 5 October 1965)

The $Ca^{46}(d,p)Ca^{47}$ reaction has been investigated using the MIT-ONR electrostatic generator. The broad-range, multiple-gap spectrograph was used in the detection of the reaction protons. Twenty-seven excited levels were identified in Ca^{47} below an excitation energy of 6.1 MeV, and a Q value of 5.047 ± 0.010 MeV was measured for the ground-state transition. The angular distributions to the corresponding levels were measured and analyzed by means of the distorted-wave Born approximation. Unperturbed single-particle energies were extracted from the strengths and energies of the levels using the shell-model sum rules. An $l_n=2$ and an $l_n=0$ transition were observed to the 2.580- and 2.600-MeV levels, respectively. The Ca^{46} ground-state configuration is discussed in terms of these results.

I. INTRODUCTION

THE level structure of Ca^{47} has been investigated by using the $Ca^{46}(d,p)Ca^{47}$ reaction at an incident deuteron energy of 7.00 MeV. The scope and the techniques of the present experiment are similar to those used by Bjerregaard *et al.*[1] who studied the $Ca^{46}(d,p)Ca^{47}$ reaction at 10-MeV bombarding energy. In the present case, 28 levels were observed in Ca^{47} below 6.1 MeV of excitation. Compared with Ref. 1, we have identified four new levels at $E_x=3.425$, 4.103, 5.220, and 5.254 MeV. Generally, the two sets of data are in excellent agreement, although in two cases the values of the transferred orbital angular momentum (l_n values) derived from the present data differ from the assignments made in Ref. 1.

The Ca^{46} target nucleus has two neutron holes relative to the doubly magic $N=28$, $Z=20$ Ca^{48} core. In principle, the transition strength to the ground state of Ca^{47} should give a measure of the degree of configuration admixing in the Ca^{46} ground state.[2] However, since the

* This work has been supported in part, through AEC Contract No. AT(30-1)-2098, with funds provided by the U. S. Atomic Energy Commission.
† On leave from the Institute for Theoretical Physics, University of Copenhagen, Copenhagen, Denmark. Present address: Rutgers, The State University, New Brunswick, New Jersey.
‡ Now at Massachusetts Institute of Technology, Cambridge, Massachusetts.
[1] J. H. Bjerregaard, Ole Hansen, and G. Sidenius, Phys. Rev. 138, B1097 (1965).
[2] M. H. Macfarlane and J. B. French, Rev. Mod. Phys. 32, 567 (1960).